Available online at www.sciencedirect.com
SCIENCE DIRECT®
International Journal of Pharmaceutics 262 (2003) 1–11
international journal of pharmaceutics
www.elsevier.com/locate/ijpharm

Fluorescence and electron microscopy probes for cellular and tissue uptake of poly(D,L-lactide-*co*-glycolide) nanoparticles

Jayanth Panyam [a], Sanjeeb K. Sahoo [a], Swayam Prabha [a], Tom Bargar [b], Vinod Labhasetwar [a,c,*]

[a] *Department of Pharmaceutical Sciences, University of Nebraska Medical Center, Omaha, NE 68198, USA*
[b] *Department of Genetics, Cell Biology and Anatomy, University of Nebraska Medical Center, Omaha, NE 68198, USA*
[c] *Department of Biochemistry and Molecular Biology, University of Nebraska Medical Center, Omaha, NE 68198, USA*

Received 24 October 2002; received in revised form 13 February 2003; accepted 16 May 2003

Abstract

Nanoparticles formulated from poly(D,L-lactide-*co*-glycolide) (PLGA) and poly(lactide) (PLA) are being extensively investigated for different therapeutic applications such as for sustained drug, vaccine, and gene delivery. For many of these applications, it is necessary to study the intracellular distribution as well as the tissue uptake of nanoparticles to optimize the efficacy of the encapsulated therapeutic agent. Fluorescence and electron microscopic techniques are usually used for the above purposes. Colloidal gold particles and fluorescent polystyrene, which are generally used as model particles for electron and fluorescence microscopy, respectively, may not be suitable alternatives to PLGA/PLA nanoparticles for these studies mainly because of the differences in their physical properties and also because they do not contain any therapeutic agent. The aim of the present study was to develop and characterize PLGA nanoparticle formulations that would be suitable for confocal/fluorescence and transmission electron microscopic (TEM) studies. Towards this objective, PLGA nanoparticles containing 6-coumarin as a fluorescent marker and osmium tetroxide as an electron microscopic marker with bovine serum albumin (BSA) as a model protein were formulated. Different physical properties of marker-loaded nanoparticles such as particle size, zeta potential, residual PVA content and protein-loading were compared with those of unloaded nanoparticles and were found to be not significantly different. Furthermore, marker-loaded nanoparticle formulations were non-toxic to the cells as unloaded nanoparticles. Nanoparticles loaded with 6-coumarin were found to be useful for studying intracellular nanoparticle uptake and distribution using confocal microscopy while osmium tetroxide-loaded nanoparticles were found to be useful for studying nanoparticle uptake and distribution in cells and tissue using TEM. It was concluded that 6-coumarin and osmium tetroxide could serve as useful fluorescence and electron microscopy probes, respectively, for incorporation into nanoparticles to study their cellular and tissue distribution.

Keywords: Drug delivery; Biodegradable polymers; Transmission electron microscopy; Confocal microscopy

1. Introduction

Nanoparticles formulated from the biocompatible and biodegradable polymers, poly(D,L-lactide-*co*-glycolide) (PLGA) and poly(lactide) (PLA), are being extensively investigated for different therapeutic applications such as for sustained drug, vaccine, and

* Corresponding author. Tel.: +1-402-559-9021; fax: +1-402-559-9543.
E-mail address: vlabhase@unmc.edu (V. Labhasetwar).

0378-5173/$ – see front matter © 2003 Elsevier B.V. All rights reserved.
doi:10.1016/S0378-5173(03)00295-3

gene delivery (Moghimi et al., 2001; Panyam and Labhasetwar, 2003a). For a number of these applications, it is important to study the kinetics of cellular and tissue uptake, intracellular distribution and retention, and in vivo biodistribution of nanoparticles (Panyam and Labhasetwar, 2003b). For example, it might be necessary to study the efficiency of nanoparticle localization in a particular cell population, organ or specific tissue following their local or systemic administration to optimize drug therapy (Lamprecht et al., 2001; Panyam et al., 2002b). Similarly, it is necessary to study the effect of various nanoparticle formulation parameters and their physical properties (e.g. surface charge, particle size) on cellular uptake of nanoparticles and their distribution in various cellular compartments (e.g. endo-lysosomes, cytoplasm, nucleus, etc.). Understanding of the intracellular and tissue distribution of nanoparticles is also useful to elucidate the mechanism of enhanced therapeutic efficacy of nanoparticle-encapsulated therapeutic agents (Demoy et al., 1999; Prabha et al., 2002; Sahoo et al., 2002; Desai et al., 1997).

For many of these applications, fluorescent polystyrene nanoparticles are used as a model for PLGA/PLA nanoparticles so that nanoparticle uptake and distribution can be visualized by either confocal or fluorescence microscopy or quantified by analyzing the extracted fluorescent dye (Zauner et al., 2001). Similarly, colloidal gold particles are used as a model for studying nanoparticle uptake and distribution by transmission electron microscopy (TEM) because of their electron dense nature (McIntosh et al., 2002). However, physical properties of these model nanoparticles including hydrophobicity, surface charge, particle size distribution, density and protein adsorption could be different from that of PLGA/PLA nanoparticles. For example, polystyrene nanoparticles are more hydrophobic than PLGA nanoparticles (Norris et al., 1999). Although polystyrene nanoparticles are available with different surface functional groups on the surface (e.g. carboxylated or amine modified), typical non-functionalized polystyrene nanoparticles have a markedly more negative zeta potential than PLGA nanoparticles due to the presence of small number of sulfate groups on the surface (Panyam et al., 2002b). Also, PLGA nanoparticles are cationic in acidic pH and anionic in neutral and alkaline pH whereas polystyrene nanoparticles are anionic in all pH values (Panyam et al., 2002b). In our recent studies, cationization of PLGA nanoparticles in the acidic pH of endo-lysosomal compartment has been demonstrated as the mechanism for their escape into cytoplasmic compartment, signifying the role of surface charge on intracellular distribution of nanoparticles (Panyam et al., 2002b). In addition, PLGA/PLA nanoparticles are typically prepared using an emulsifier (e.g. polyvinyl alcohol, PVA). Recently, we have shown that residual PVA associated with PLGA nanoparticles significantly affects their interfacial as well as cellular uptake properties (Sahoo et al., 2002). The results of the above study thus suggest the importance of interfacial properties of nanoparticles towards their interaction with cells. Further, no therapeutic agent can be encapsulated in the above model nanoparticles, which could also affect the surface properties of nanoparticles. Hence, the results obtained with polystyrene or gold nanoparticles might not truly represent what would be seen with PLGA/PLA nanoparticles.

To overcome this problem, studies by other investigators have attempted to use radiolabeled-polymer for formulating nanoparticles and then quantify the radioactivity to follow the uptake and distribution (Le Ray et al., 1994). However, the limitation of this approach is that the uptake and distribution of these nanoparticles in different intracellular compartments or uptake by a particular cell population in a tissue sample cannot be followed by microscopic techniques. Furthermore, for studies using TEM, cell and tissue contain many vesicles, which look like nanoparticles, and oftentimes, it is difficult to distinguish them from nanoparticles, as PLGA or PLA are not electron dense polymers.

The aim of the present study was to identify suitable probes that can be incorporated into nanoparticles along with a therapeutic agent that would be suitable for confocal/fluorescence microscopy and TEM studies. Bovine serum albumin (BSA) was used as a model protein for encapsulation in nanoparticles. We have characterized 6-coumarin, a lipophilic fluorescent dye, incorporated in nanoparticles as a marker for confocal microscopy to study nanoparticle uptake in cells. Similarly, we have determined the suitability of osmium tetroxide, an electron dense agent, incorporated in nanoparticles as a marker to study nanoparticle uptake in cells and tissues using TEM.

2. Materials and methods

2.1. Materials

BSA (Fraction V) and PVA (average molecular weight, 30,000–70,000) were purchased from Sigma (St. Louis, MO). LysoTracker® Red was purchased from Molecular Probes (Eugene, OR). 6-Coumarin was purchased from Polysciences (Warrington, PA). PLGA (50:50 lactide–glycolide ratio, 143,000 Da) was purchased from Birmingham Polymers (Birmingham, AL). All the reagents used for TEM were from Electron Microscopy Services (Ft. Washington, PA).

2.2. Methods

2.2.1. Nanoparticle formulation

Nanoparticles containing BSA and 6-coumarin were formulated using a double emulsion-solvent evaporation technique as described previously (Davda and Labhasetwar, 2002). An aqueous solution of BSA (60 mg/ml, 1 ml) was emulsified in a PLGA solution (180 mg in 6 ml chloroform) containing 6-coumarin (100 μg) using a probe sonicator (55 W for 2 min) (Sonicator® XL, Misonix, NY). The water-in-oil emulsion formed was further emulsified into 50 ml of 2.5% w/v aqueous solution of PVA by sonication (55 W for 5 min) to form a multiple water-in-oil-in-water emulsion. The multiple emulsion was stirred for ∼18 h at room temperature followed by for 1 h in a desiccator under vacuum to remove the residual chloroform. Nanoparticles were recovered by ultracentrifugation (35,000 rpm for 20 min at 4 °C, Optima™ LE-80K, Beckman, Palo Alta, CA), washed two times with distilled water to remove PVA, unentrapped BSA and 6-coumarin, and then lyophilized (−80 °C and <10 μm mercury pressure, Sentry™, Virtis, Gardiner, NY) for 48 h to obtain a dry powder. Nanoparticles containing osmium tetroxide were formulated similarly, except, instead of 6-coumarin, 10 mg osmium tetroxide was added to the polymer solution prior to emulsification. Dry lyophilized nanoparticle samples were stored in a dessicator at 4 °C and were reconstituted in a suitable medium (buffer or cell culture medium) prior to an experiment.

2.2.2. Nanoparticle characterization

2.2.2.1. Particle size and surface charge (zeta potential). Particle size and size distribution were determined by photon correlation spectroscopy (PCS) using quasi-elastic light scattering equipment (ZetaPlus™ equipped with particle sizing mode, Brookhaven Instrument Crop., Holtsville, NY). A dilute suspension (100 μg/ml) of nanoparticles was prepared in double distilled water and sonicated on an ice bath for 30 s. The sample was subjected to particle size analysis. Zeta potential of nanoparticles in 0.001 M HEPES buffer, pH 7.4 (0.5 mg/ml) was determined using ZetaPlus™ in the zeta potential analysis mode.

2.2.2.2. Protein loading. Amount of BSA encapsulated in nanoparticles was determined by analyzing the protein content in the washings from the nanoparticle formulation step. Protein content was measured using BCA protein assay kit (Pierce, Rockford, IL). Protein loading in nanoparticles was calculated by subtracting the amount of protein present in the washings from the total protein added.

2.2.2.3. Residual PVA content. Residual amount of PVA associated with nanoparticles was determined by a colorimetric method (Sahoo et al., 2002). In brief, 2 mg of lyophilized nanoparticle sample was treated with 2 ml of 0.5 M NaOH for 15 min at 60 °C. Samples were neutralized with 900 μl of 1N HCl and the volume was adjusted to 5 ml with distilled water. To each sample, 3 ml of a 0.65 M solution of boric acid, 0.5 ml of I_2/KI (0.05/0.15 M) solution, and 1.5 ml of distilled water were added. Finally, the visible spectra absorbance of the samples was measured at 690 nm (UV-1601PC UV-Vis Spectrophotometer, Shimadzu Scientific Instruments, Columbia, MD) after 15 min incubation. A standard plot of PVA was prepared under identical conditions.

2.2.2.4. In vitro release of 6-coumarin. To determine the amount of 6-coumarin released from nanoparticles under different pH conditions, nanoparticles were incubated with 0.1 M HEPES buffer of pH 4 and 7.4. Buffers of pH 4 and 7.4 were selected for the in vitro release studies to represent the pH present in the endo-lysosomal compartment and physiologic pH, respectively. About 1 mg of 6-coumarin-loaded nanoparticles was dispersed in 0.5 ml of HEPES

buffer, which was then placed inside a Spectra/Por® CE cellulose ester DispoDialyzer dialysis bags (300,000 Da molecular weight cut-off, Pierce). Each dialysis bag was then placed in 9.5 ml of HEPES buffer contained in 15 ml centrifuge tubes (Becton Dickinson). The whole set up was then incubated at 37 °C and shaken at 100 rpm (Environ® orbital shaker, Lab Line, Melrose Park, IL). Samples (1.0 ml) were taken from outside the dialysis bag and replaced with fresh buffer. Samples were lyophilized (−80 °C and <10 μm mercury pressure, Sentry™, Virtis) and then reconstituted in 1 ml methanol. Amount of 6-coumarin in the release samples was analyzed by our previously reported HPLC method (Davda and Labhasetwar, 2002). Care was taken to protect the samples from light throughout the experimental procedure.

2.2.3. Biocompatibility studies

Human vascular smooth muscle cells (abbreviated as VSMCs, Cascade Biologics, Portland, OR) cultured in Medium 231 with added smooth muscle growth supplement (Cascade Biologics) and 100 μg/ml penicillin G and 100 μg/ml streptomycin (Gibco BRL, Grand Island, NY), were used for all the cell culture studies. The cells were seeded at 5000 cells per well/0.1 ml (50% confluency) in a 96-well plate and allowed to attach overnight. Marker-loaded nanoparticles were added at different doses in 0.1 ml of the medium and incubated for 2 days. Untreated cells (plain medium) were used as a control. Polyethylenimine (25 kDa, Aldrich, Milwaukee, WI) was used a positive control for the assay. At the end of the incubation period, cells were washed twice with phosphate buffered saline (PBS, pH 7.4) to remove nanoparticles and 0.1 ml of fresh medium was added to each well. The viability of the cells was determined using MTS assay (CellTiter 96 AQ_{ueous}, Promega, Madison, WI). The MTS reagent (20 μl) was added to each well, incubated for 150 min and the absorbance was measured at 490 nm using a microplate reader (BT 2000 Microkinetics Reader, BioTek Instruments, Inc., Winooski, VT).

2.2.4. Confocal microscopic studies

VSMCs were plated in Bioptech® plates (Bioptechs, Butler, PA) at 50,000 cells per plate (50% confluency) in 1 ml of growth medium and allowed to attach for 24 h. Cells were then incubated with 6-coumarin-loaded nanoparticle suspension (100 μg/ml) in growth medium for 60 min. Cells were then washed twice with PBS and visualized with HEPES buffer (pH 8) using a Zeiss Confocal LSM410 microscope equipped with Argon–Krypton laser (Carl Zeiss Microimaging, Inc., Thornwood, NY).

2.2.5. TEM studies

TEM of control nanoparticles was performed by negative staining with uranyl acetate. A drop of nanoparticle suspension (1 mg/ml) was placed on Formvar®-coated copper grids (150 mesh, Ted Pella Inc., Redding, CA) and allowed to equilibrate. Excess liquid was removed with a filter paper and a drop of 2% w/v uranyl acetate was added to the grid. After 3 min of incubation at room temperature, excess liquid was removed and the grid was air-dried. The dried grid containing the nanoparticles was visualized using a Philips 201® transmission electron microscope (Philips/FEI Inc., Briarcliff Manor, NY). Osmium tetroxide-loaded nanoparticles were visualized without the negative staining.

For cell uptake studies, VSMCs were plated 24 h prior to the experiment in 100-mm tissue culture dishes (Becton Dickinson) at 500,000 cells per dish in 10 ml of growth medium. Cells were incubated with osmium tetroxide-loaded nanoparticle suspension (100 μg/ml) and were washed twice with PBS at 1 h post incubation. Cells were harvested by trypsinization and then fixed in a 2.5% glutaraldehyde solution in PBS for 1 h and then post-fixed in 1% osmium tetroxide in PBS for 1 h. Fixed cells were washed with Sörenson's PBS and dehydrated three times sequentially in a graded series of ethanol solutions (50, 70, 90, 95, and 100%); they were then soaked overnight in a 1:1 ratio of 100% ethyl alcohol and Unicryl® embedding resin (Ted Pella Inc.), and then in fresh Unicryl® resin for 4–5 h. The resin-embedded cells were placed in BEEM capsules (EMS), and the capsules were placed in a Pelco UV-2 Cryo Chamber (Ted Pella Inc.) at 4 °C for 48 h for polymerization of the resin by UV radiation. The polymerized blocks were sectioned and the sections (80–100 nm thick) were placed on Formvar®-coated copper grids (150 mesh, Ted Pella Inc.), stained with an aqueous solution of 2% uranyl acetate for 15 min, washed briefly in water, stained with Reynold's lead citrate for 7 min, and then finally washed in water prior to visualization under a Philips 210® microscope (Philips/FEI Inc.).

Table 1
Physical characterization of marker-loaded PLGA nanoparticles

Nanoparticles with or without markers	Particle size ± S.E.M. (nm)[a] ($n = 5$)	Zeta potential ± S.E.M. (mV)[b] ($n = 5$)	Protein loading (% w/w)	Encapsulation efficiency (%) of protein	Percent of residual PVA content (w/w)	Marker loading (% w/w)[c]
6-Coumarin	263 ± 6	−12.6 ± 1.4	22.3	66	4.6 ± 0.2	0.05
Osmium tetroxide	297 ± 12	−10.6 ± 1.4	19.2	57	5.5 ± 0.4	nd
Without marker	267 ± 10	−7.9 ± 1.8	17.8	53	4.2 ± 0.4	–

[a] Mean hydrodynamic diameter measured by photon correlation spectroscopy.
[b] Measured in 0.001 M HEPES buffer, pH 7.4.
[c] nd: not determined.

For tissue distribution studies, male athymic nude mice (2–3 weeks age, 20–30 g weight, Charles River Laboratories, Wilmington, MA) were used. Animals were maintained in a pathogen-free environment and handled according to the *Guide for the Care and Use of Laboratory Animals* published by the U.S. National Institutes of Health (NIH Publication No. 85-23, revised 1996) and the ethical guidelines of the University of Nebraska Medical Center Institutional Animal Care and Use Committee.

Osmium tetroxide-loaded nanoparticles were suspended in Hank's balanced salt solution (1 mg/ml) and injected intramuscularly into the left thigh of the animal (200 μl per animal). Right thigh muscles were injected with vehicle and were used as controls. One hour following the injection, mice were euthanized and the muscle tissue samples were collected, cut into ∼1 mm^3 pieces and then fixed in 2.5% glutaraldehyde solution in PBS. Post-fixation, embedding, sectioning, and staining procedures were performed similar to that described for cell culture samples.

3. Results and discussion

3.1. Nanoparticle characterization

Table 1 describes the physical characterization of different nanoparticle formulations. All the nanoparticle formulations had a mean diameter in the size range

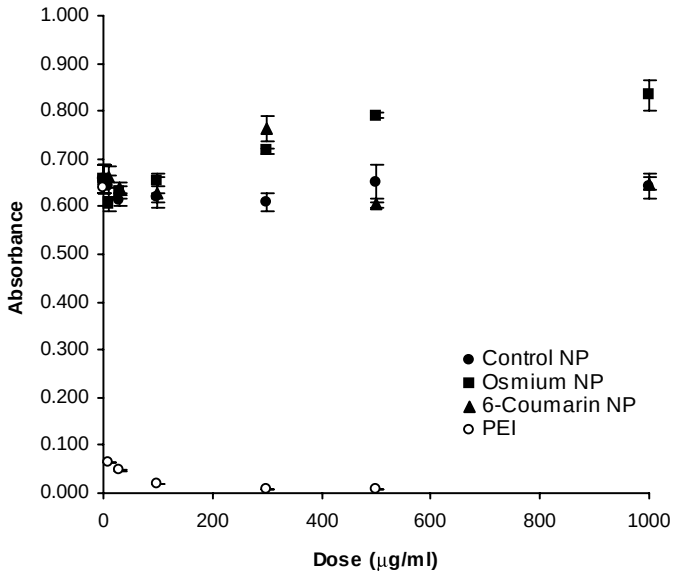

Fig. 1. Biocompatibility of marker-loaded nanoparticles. VSMCs were incubated with different doses of nanoparticles and the viability of the cells was determined by MTS assay. Polyethylenimine was used as a positive control.

of 250–300 nm with log normal size distribution as measured by dynamic light scattering and had a zeta potential in the range of −7.9 to −12.6 mV at pH 7.4. The percent of residual PVA was in the range of 4.2–5.5% w/w. All the nanoparticle formulations had similar protein loading, the range being 18–22% w/w.

Previous studies have shown that particle size is an important property that affects t he intracellular uptake of nano- and microparticles, with smaller size particles, in general, having higher uptake (Desai et al., 1997). Particle size could also affect the efficacy of nanoparticle-encapsulated therapeutic agents. We have shown that smaller size nanoparticles have higher transfectivity compared to larger size nanoparticles in vitro (Prabha et al., 2002). Similarly, we have shown that zeta potential of nanoparticles plays an important role in affecting the intracellular trafficking of nanoparticles. Nanoparticles that show a reversal in their zeta potential (from anionic to cationic) in acidic pH (e.g. PLGA nanoparticles) can escape the degradative endo-lysosomal compartment into the cytosol, whereas nanoparticles that remain anionic at all pH values (e.g. polystyrene nanoparticles) do not exhibit endo-lysosomal escape (Panyam et al., 2002b). Further, we have shown that residual PVA content of nanoparticles affects the cellular uptake properties of nanoparticles, with nanoparticles containing lower amounts of residual PVA demonstrating higher uptake (Sahoo et al., 2002). Thus, the above physical characteristics of nanoparticles are important in determining their intracellular uptake and trafficking of nanoparticles. As seen from Table 1, nanoparticles containing the markers had similar physical characteristics as that of nanoparticles without any marker.

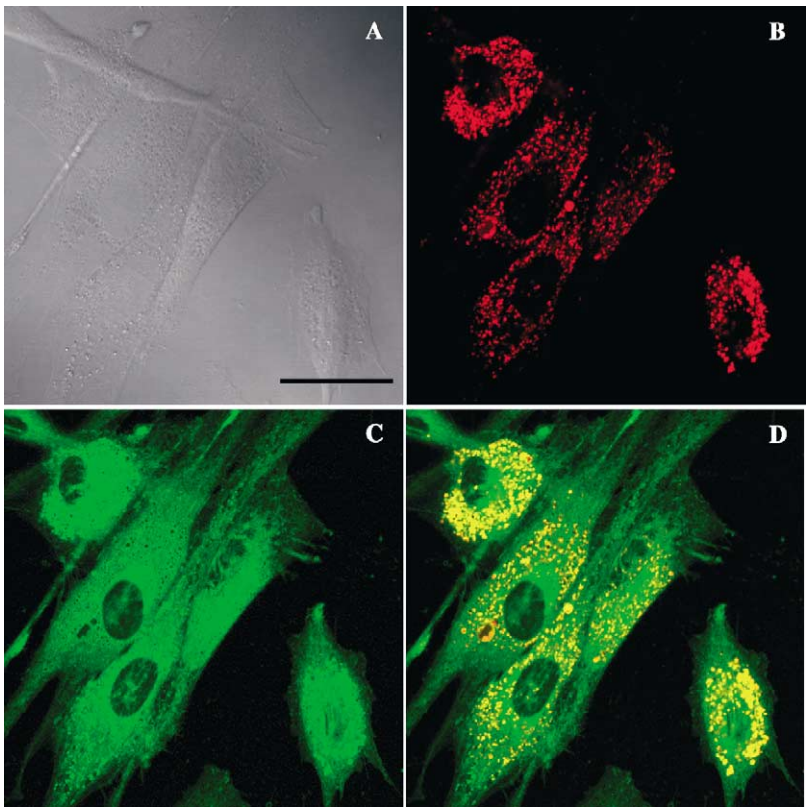

Fig. 2. Confocal microscopic images demonstrating the intracellular distribution of 6-coumarin-loaded nanoparticles in VSMCs. (A) Differential interference contrast image showing the outline of the cells. (B) Cells stained with LysoTracker® Red and visualized using RITC filter. (C) Uptake of green fluorescent 6-coumarin-loaded nanoparticles in VSMCs visualized using FITC filter. (D) Overlay of (B) and (C) showing the co-localization of nanoparticles with endo-lysosomes. Bar represents 25 μm.

One concern in using osmium tetroxide and 6-coumarin as markers for nanoparticles is their biocompatibility. Osmium tetroxide is known to be toxic and is a potent irritant. Nanoparticles should therefore not release the marker in significant amounts during the time period of the study, which could result in acute toxicity. Hence, we tested the biocompatibility of marker-loaded nanoparticles in cell culture. As seen from Fig. 1, there was no acute toxicity associated with either 6-coumarin- or osmium tetroxide-loaded nanoparticles compared to either control nanoparticle-treated or untreated (plain medium) cells. Polyethylenimine, a commonly used gene transfection reagent (Boussif et al., 1995), showed significant cytotoxicity in the concentration range tested (~80% toxicity at 2 μg/ml dose).

3.2. 6-Coumarin-loaded nanoparticles for fluorescence microscopy

Nanoparticles loaded with 6-coumarin were characterized for the leaching of dye in two different pH buffers. We have previously shown that under physiological conditions such as in pH 7.4 buffer or in the presence of lipids (to simulate membrane lipids), less than 0.5% of the dye is released, suggesting the suitability of 6-coumarin as a marker for nanoparticles (Desai et al., 1996; Davda and Labhasetwar, 2002). However, recent studies have shown that nanoparticles, following their intracellular uptake, are trafficked through an acidic endo-lysosomal compartment (pH 4–5) (Panyam et al., 2002b). Hence, it is pertinent to test the release of the dye in acidic pH to ensure that green fluorescence seen inside the cells in confocal microscopy (Fig. 2) is not due to the dye released in acidic pH. About 0.10% of the encapsulated dye was released in pH 4 compared to about 0.45% release observed in pH 7.4 in 48 h (Fig. 3), suggesting that dye is not released in acidic pH present in endo-lysosomes. Thus, 6-coumarin has the advantage over other dyes which show pH-dependent solubility. For example, rhodamine forms a water-soluble salt in acidic pH (ref. Merck Index, 12th edition) and hence, the dye could be released from nanoparticles in the endo-lysosomes, which could result in inaccurate intracellular distribution pattern.

From the above results, it can be seen that 6-coumarin could be a useful probe for fluorescence/confocal microscopic studies. The other advantages

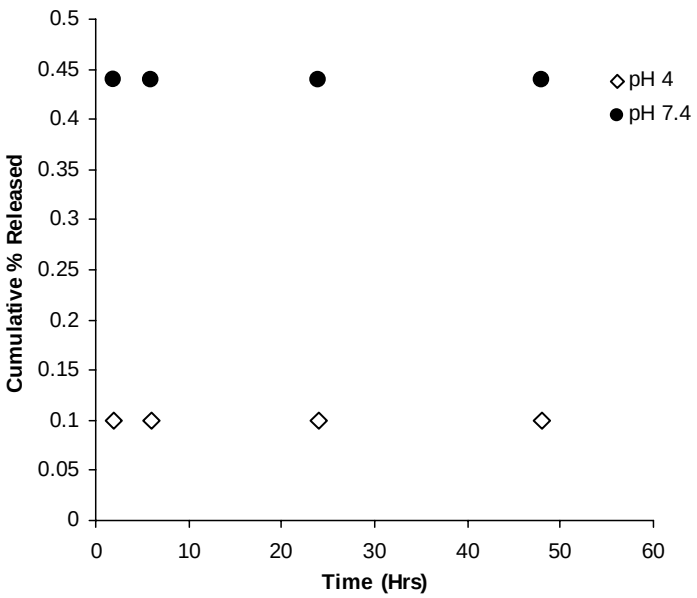

Fig. 3. In vitro release of 6-coumarin from nanoparticles in HEPES buffer (0.15 M) of pH 4 and 7.4. Standard deviations were less than 1% in all the cases.

of 6-coumarin include the requirement of low dye loading in nanoparticles due to its high fluorescence activity. About 0.05% w/w dye loading in the particles results in brightly fluorescent nanoparticles (Fig. 2). The uptake of these nanoparticles can be easily visualized by confocal microscopy. Most cells that were tested (VSMCs, vascular endothelial cells, COS-7 and HEK-293) do not have background fluorescence in the fluorescence emission range of 6-coumarin. Another advantage of 6-coumarin is the possibility of its quantitation by HPLC. We have previously reported a sensitive HPLC method to quantitate 6-coumarin in both cell lysates and in tissue samples (Panyam et al., 2002a; Davda and Labhasetwar, 2002). The assay is sensitive, with detection limit of 5 ng of nanoparticles. Also, due to its high lipid solubility, dye can be extracted from cell lysates and tissue samples using organic solvents such as methanol or ethyl acetate with extraction efficiency close to 95%.

6-Coumarin-labeled nanoparticles can be used to study the intracellular distribution by using co-localization techniques. Using an organelle-specific dye with contrasting fluorescence, it is possible to study the co-localization of nanoparticles in the particular organelle. For example, using LysoTracker® Red, a pH sensitive dye that emits red fluorescence in acidic pH, and 6-coumarin-loaded nanoparticles, it was possible to determine the presence of nanoparticles in the acidic endo-lysosomal vesicles. Presence of green fluorescent nanoparticles in red fluorescent vesicles shows up as yellow fluorescence in the over-

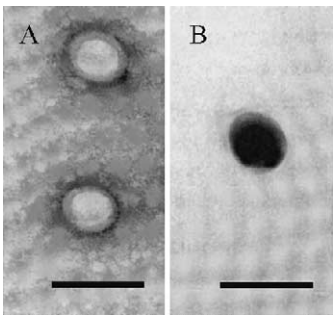

Fig. 4. TEM images of (A) control (blank) nanoparticles and (B) osmium tetroxide-loaded nanoparticles. Control nanoparticles were visualized following negative staining with 2% w/v uranyl acetate. Bar represents 250 nm (31,000× magnification).

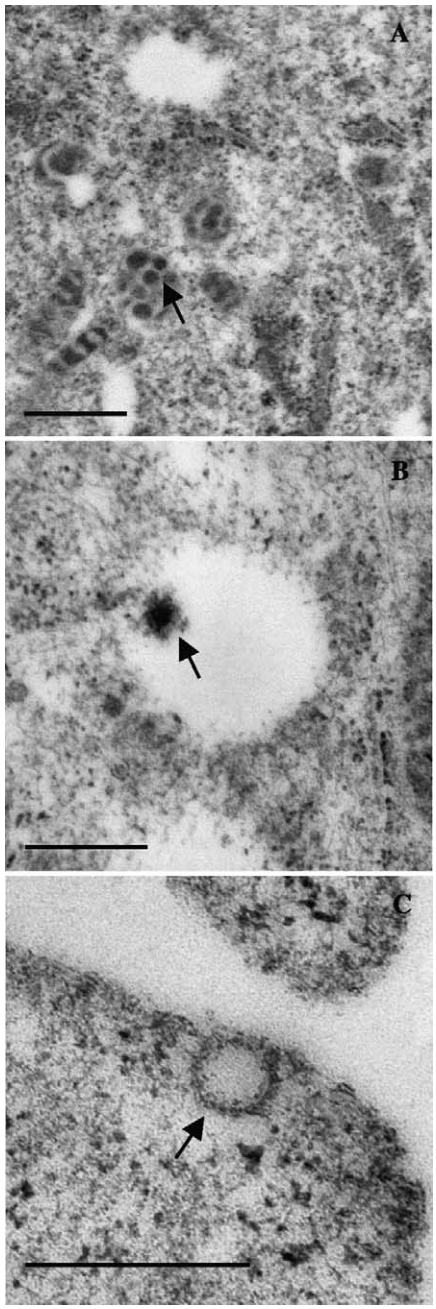

Fig. 5. TEM images showing (A) nanoparticles (indicated by arrow) present in the cytoplasm (16,900×), (B) a nanoparticle (indicated by arrow) interacting with vesicular membrane (21,000×), and (C) control VSMCs (untreated cells) with nanoparticle-like vesicles of approximately 100 nm (indicated by arrow) (38,000×). Bars represent 500 nm.

lay (Fig. 2). The same approach can be used to study the co-localization of nanoparticles in other organelles such as the nucleus or mitochondria using specific fluorescent dyes.

6-Coumarin-loaded nanoparticles can also be used for acute in vivo pharmacokinetics and tissue distribution studies. These nanoparticles were used in our previous studies for comparing the efficiency of two infusion catheters in localizing nanoparticles in balloon-injured artery (Panyam et al., 2002a). Also nanoparticle distribution in arterial section was determined using fluorescence microscopy. Thus, using 6-coumarin as a marker, the differences in the nanoparticle distribution in different tissue can be visualized as well as their levels quantitated.

3.3. Osmium tetroxide-loaded nanoparticles for electron microscopy

Previous approaches to study the tissue or intracellular distribution of nanoparticles by electron microscopy have mostly used gold or gold-labeled particles (McIntosh et al., 2002) since gold is electron-dense and gold particles are available in pre-defined sizes. However, being metallic in nature, gold particles would have widely different properties compared to that of polymer particles used in drug delivery. Hence, osmium tetroxide was investigated as an electron microscopy marker for PLGA nanoparticles. Osmium tetroxide is an electron dense agent that has been previously used for post-fixation and

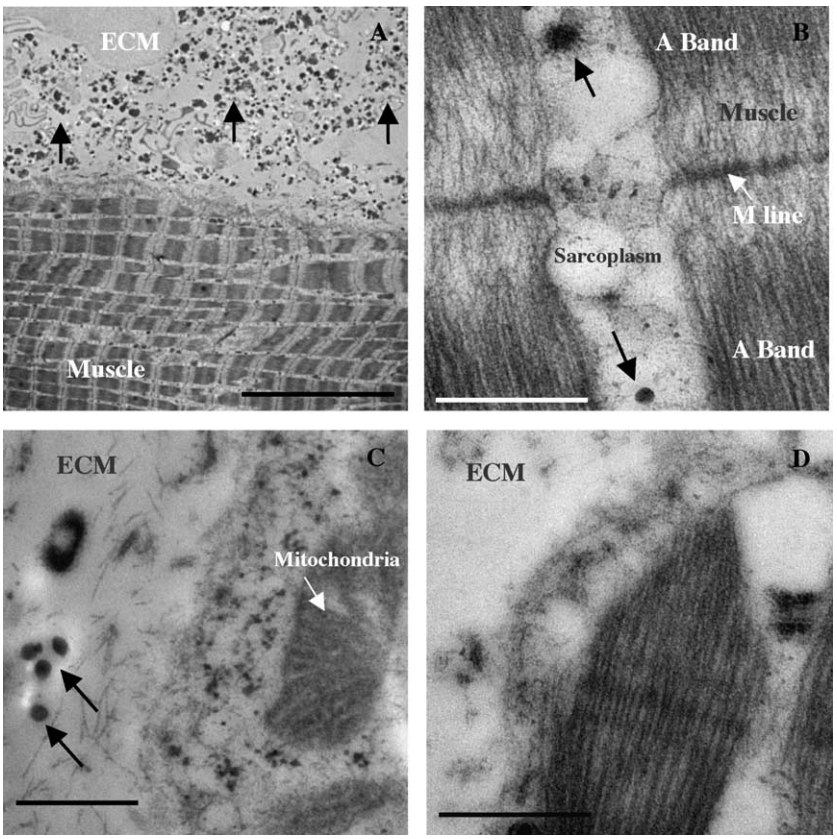

Fig. 6. (A) Low magnification TEM image (1600×) of muscle tissue showing nanoparticles (indicated by arrows) mainly in ECM and some in the muscle fibers. (B) Higher magnification (31,000×) image showing the presence of nanoparticles in the sarcoplasm of the muscle cell (indicated by black arrow). Dark band (A band) and M line can be seen in the muscle fibril. (C) Nanoparticles (black arrow) can be easily distinguished from other intracellular structures like mitochondria (striated structure, white arrow) at high magnifications (31,000×). (D) TEM image of control tissue from the uninjected thigh muscle (31,000×). In (A) bar represents 10 μm whereas in (B), (C) and (D), bar represents 500 nm.

staining cells for transmission electron microscopy. It has high affinity for lipids and hence has been used for staining lipids in cells and tissue. Because of its solubility in organic solvents, osmium tetroxide can be easily dissolved along with the polymer solution prior to emulsification.

Fig. 4 shows the transmission electron microscopic images of control nanoparticles and osmium tetroxide-loaded nanoparticles. The control particles required negative staining with uranyl acetate to be visible under an electron beam while osmium tetroxide particles are visible without any staining due to the electron dense nature of osmium tetroxide. It was possible to clearly distinguish the nanoparticles within the cellular compartments because of their distinct dark color (Fig. 5A and B). PLGA nanoparticles without any marker could not be used to study the intracellular uptake and localization of nanoparticles since it was difficult to distinguish between intracellular vesicles from nanoparticles (Fig. 5C).

In order to determine the suitability of osmium tetroxide-loaded nanoparticles for studying tissue distribution using TEM, these particles were injected into mouse thigh muscle. Following intramuscular administration, a major fraction of the nanoparticles was found in the extracellular matrix of the muscle tissue (Fig. 6A). It is possible that the negatively charged nanoparticles are attracted to cationic molecules such as proteoglycans in the ECM. However, it is expected that this phenomenon would be similar for all the PLGA nanoparticle formulations since all of them have similar negative zeta potential values (Table 1). Some nanoparticles were taken up by the muscle cells and were found in the sarcoplasm (Fig. 6B). Nanoparticles could be identified as dark spherical structures, about 100–200 nm in size. At lower magnification, it was difficult to distinguish nanoparticles from mitochondria since they are also dark colored structures. However, at higher magnification, mitochondria could be easily distinguished due to their shape, size and the presence of distinct striations (Fig. 6C). Control tissue did not show black spherical structures (Fig. 6D).

4. Limitations

While these microscopy markers have been shown to be useful in acute studies, their usefulness in chronic studies is not yet determined. Although <1% of 6-coumarin leaches out from nanoparticles in aqueous medium over a 48 h period, the in vivo or intracellular fate of the dye over a longer time period is yet to be studied. Similarly, osmium tetroxide-loaded particles did not demonstrate any toxicity over a period of 2 days, however, their long-term biocompatibility is not known.

5. Conclusions

We have characterized nanoparticles containing 6-coumarin and osmium tetroxide as fluorescent and transmission electron microscopic probes, respectively. The formulation characteristics of nanoparticles containing the probes were similar to that of unloaded nanoparticles. Encapsulation of the markers did not affect the biocompatibility of nanoparticles. It can be concluded that these nanoparticles could serve as useful probes for studying nanoparticle uptake, retention and distribution in vivo and in vitro.

Acknowledgements

Grant support from the National Institutes of Health (HL 57234) and the Nebraska Research Initiative, Gene Therapy Program. J.P. and S.S. are supported by pre-doctoral and post-doctoral fellowships from the American Heart Association. Predoctoral fellowship to S.P. (DAMD-17-02-1-0506) from Department of Army, the U.S. Army Medical Research Association Activity, 820 Chandler Street, Fort Detrick, MD 21702-5014. We would like to thank Janice Taylor, confocal laser microscopy core facility at UNMC, for her assistance with the microscopic studies and Ms. Elaine Payne for providing administrative assistance. We would like to thank the core electron microscopy facility, Department of Genetics, Cell Biology and Anatomy, UNMC, for assistance with TEM studies.

References

Boussif, O., Lezoualc'h, F., Zanta, M.A., Mergny, M.D., Scherman, D., Demeneix, B., Behr, J.P., 1995. A versatile vector for gene and oligonucleotide transfer into cells in culture and in vivo:

polyethylenimine. Proc. Natl. Acad. Sci. U.S.A. 92, 7297–7301.

Davda, J., Labhasetwar, V., 2002. Characterization of nanoparticle uptake by endothelial cells. Int. J. Pharm. 233, 51–59.

Demoy, M., Andreux, J.P., Weingarten, C., Gouritin, B., Guilloux, V., Couvreur, P., 1999. Spleen capture of nanoparticles: influence of animal species and surface characteristics. Pharm. Res. 16, 37–41.

Desai, M.P., Labhasetwar, V., Amidon, G.L., Levy, R.J., 1996. Gastrointestinal uptake of biodegradable microparticles: effect of particle size. Pharm. Res. 13, 1838–1845.

Desai, M.P., Labhasetwar, V., Walter, E., Levy, R.J., Amidon, G.L., 1997. The mechanism of uptake of biodegradable microparticles in Caco-2 cells is size dependent. Pharm. Res. 14, 1568–1573.

Lamprecht, A., Schafer, U., Lehr, C.M., 2001. Size-dependent bioadhesion of micro- and nanoparticulate carriers to the inflamed colonic mucosa. Pharm. Res. 18, 788–793.

Le Ray, A.M., Vert, M., Gautier, J.C., Benoit, J.P., 1994. End-chain radiolabeling and in vitro stability studies of radiolabeled poly(hydroxy acid) nanoparticles. J. Pharm. Sci. 83, 845–851.

McIntosh, D.P., Tan, X.Y., Oh, P., Schnitzer, J.E., 2002. Targeting endothelium and its dynamic caveolae for tissue-specific transcytosis in vivo: a pathway to overcome cell barriers to drug and gene delivery. Proc. Natl. Acad. Sci. U.S.A. 99, 1996–2001.

Moghimi, S.M., Hunter, A.C., Murray, J.C., 2001. Long-circulating and target specific nanoparticles: theory to practice. Pharmacol. Rev. 53, 283–318.

Norris, D.A., Puri, N., Labib, M.E., Sinko, P.J., 1999. Determining the absolute surface hydrophobicity of microparticulates using thin layer wicking. J. Control Release 59, 173–185.

Panyam, J., Labhasetwar, V., 2003a. Biodegradable nanoparticles for drug and gene delivery to cells and tissue. Adv. Drug Deliv. Rev. 55, 329–347.

Panyam, J., Labhasetwar, V., 2003b. Dynamics of endocytosis and exocytosis of poly(D,L-lactide-*co*-glycolide) nanoparticles in vascular smooth muscle cells. Pharm. Res. 20, 210–218.

Panyam, J., Lof, J., O'Leary, E., Labhasetwar, V., 2002a. Efficiency of Dispatch® and Infiltrator® cardiac infusion catheters in arterial localization of nanoparticles in a porcine coronary model of restenosis. J. Drug Target 10, 515–523.

Panyam, J., Zhou, W.Z., Prabha, S., Sahoo, S.K., Labhasetwar, V., 2002b. Rapid endo-lysosomal escape of poly(D,L-lactide-*co*-glycolide) nanoparticles: implications for drug and gene delivery. FASEB J. 16, 1217–1226.

Prabha, S., Zhou, W.Z., Panyam, J., Labhasetwar, V., 2002. Size-dependency of nanoparticle-mediated gene transfection: studies with fractionated nanoparticles. Int. J. Pharm. 244, 105–115.

Sahoo, S.K., Panyam, J., Prabha, S., Labhasetwar, V., 2002. Residual polyvinyl alcohol associated with poly(D,L-lactide-*co*-glycolide) nanoparticles affects their physical properties and cellular uptake. J. Control Release 82, 105–114.

Zauner, W., Farrow, N.A., Haines, A.M., 2001. In vitro uptake of polystyrene microspheres: effect of particle size cell line and cell density. J. Control Release 71, 39–51.